Title:	**Seismic Performance of High-Rise Intermediate Steel Moment Frames**
Authors:	Sang Whan Han, Hanyang University Ki-Hoon Moon, Daewoo Sung Jin Ha, Hanyang University
Subject:	Seismic
Keywords:	Performance Based Design Seismic Steel Structure
Publication Date:	2015
Original Publication:	International Journal of High-Rise Buildings 2015 Number 1
Paper Type:	1. Book chapter/Part chapter 2. **Journal paper** 3. Conference proceeding 4. Unpublished conference paper 5. Magazine article 6. Unpublished

International Journal of High-Rise Buildings
March 2015, Vol 4, No 1, 45-55

International Journal of
High-Rise Buildings
www.ctbuh-korea.org/ijhrb/index.php

Seismic Performance of High-Rise Intermediate Steel Moment Frames according to Rotation Capacities of Moment Connections

Sang Whan Han[1,†], Ki-Hoon Moon[2], and Sung Jin Ha[3]

[1]*Department of Architectural Engineering, Hanyang University, Seoul 133-791, Korea*
[2]*Disaster Prevention Research Team, Daewoo Institute of Construction Technology, Suwon 440-210, Korea*
[3]*Graduate student, Department of Architectural Engineering, Hanyang University, Seoul 133-791, Korea*

Abstract

The rotation capacity of the moment connections could significantly influence on the seismic performance of steel moment resisting frames. Current seismic provisions require that beam-to-column connections in Intermediate Moment Frames (IMF) should have a drift capacity as large as 0.02 radian. The objective of this study was to evaluate the effect of the rotation capacity of moment connections on the seismic performance of high-rise IMFs. For this purpose, thirty- and forty-story high-rise IMFs were designed according to the current seismic design provisions. The seismic performance of designed model frames was evaluated according to FEMA P695. This study showed that the forty-story IMF satisfied the seismic performance objective specified in FEMA P695 when the rotation capacity of the connections was larger than 0.02. However, thirty-story IMFs satisfied the performance objective when the connection rotation capacity is larger than 0.03.

Keywords: Intermediate moment frames, Rotation capacity, Performance evaluation, High-rise buildings, Moment connection

1. Introduction

The steel moment resisting frame is widely used for seismic force-resisting system as having excellent seismic performance capacity. The seismic performance of steel moment resisting frame may be significantly influenced from the ductility and energy dissipation capacity of moment connection. According to AISC/ANSI 341-10 (2010), moment frames are classified into special, intermediate and ordinary moment frames (SMF, IMF, OMF) depended on inelastic deformation capacity. And the moment frame which has superior rotation capacity requires higher response modification factor (R). The minimum rotation capacities for SMFs and IMFs are 0.04 and 0.02rad respectively and OMFs require only minimal level of inelastic rotation.

After the 1994 Northridge earthquake, numerous studies were conducted for evaluating the rotation capacities of moment connections. FEMA-355C (2000) summarizes an extensive series of analytical investigations into the demands induced in steel moment-frame buildings designed to various criteria, when subjected to a range of different ground motions. FEMA-355E (2000) and FEMA-355F (2000) conducted seismic performance evaluation of various steel moment resisting frames; existing buildings, new buildings and damaged buildings etc.

†Corresponding author: Sang Whan Han
Tel: +82-2-2220-1715; Fax: +82-2-2291-1716
E-mail: swhan82@gmail.com

The requirements of Building Code for moment frames such as limits of rotation capacities and response modification factors were results of these researches. In particular, many experimental researches were conducted for developing pre-qualified SMF connections. However, only limited studies were conducted to evaluate the seismic performance of IMFs with respect to the rotation capacity of their connections. So it is not easy to guarantee the satisfactory seismic performance of IMFs according to rotation capacity.

Han et al. (2013) reported that the seismic performance of 9- and 20-story IMFs with reduced beam section-bolted shear tab (RBS-B) moment connections failed to meet the performance criteria specified in FEMA P695 (2009). In particular, the study states that 20 story IMFs are very vulnerable on seismic performance capacities. Therefore, the seismic performance of the high-rise IMFs can be very vulnerable if the rotation capacities of moment connection are lower.

In this study, the seismic performance evaluation of 30-story and 40-story high-rise IMFs having different rotation capacity of moment connection was conducted according to FEMA P695 (2009). For this purpose, a number of IMFs were designed for seismic design category (SDC) C using design forces determined in accordance with ASCE 7-10 (2010). The seismic performance evaluation was repeated for different rotation capacities of 0.01, 0.02, 0.03 and 0.04rad to find required rotation capacity of IMFs which meets the performance criteria specified in FEMA P695 (2009).

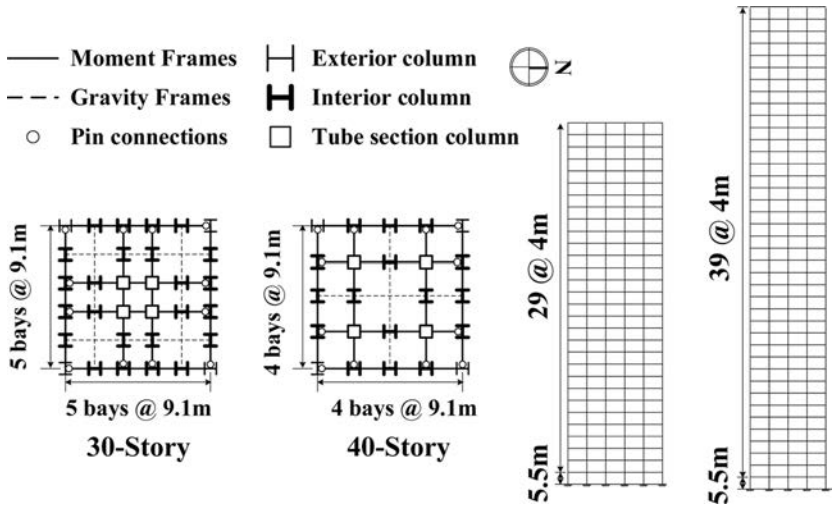

Figure 1. Floor plans and elevations for model buildings.

2. Model Frames

For conducting seismic performance evaluation for high-rise IMF system, model frames were designed according to ASCE 7-10 (2010) considering various important design parameters such as the number of stories and seismic design category. To investigate the effect of the design parameter on the seismic performance of the high-rise IMF system, the model buildings with the same design parameters are grouped, which is named 'performance group'.

This study considered two different numbers of stories (30 and 40 story) for high-rise building. The selected seismic design category (SDC) was *C* category because there is no height limitation on IMFs for SDC *C*. The design spectral acceleration parameters at short period (S_{DS}) and at 1-s period (S_{D1}) for model frames were considered for possible maximum and minimum seismic criteria of SDC: SDC C_{min} (S_{DS}=0.33g, S_{D1}=0.133g) and SDC C_{max} (S_{DS}=0.50g, S_{D1}=0.20g) where g is the gravitational acceleration.

The model frames were assumed to be used in office buildings located at a site with soil condition D according to ASCE 7-10 (2010). Fig. 1 shows floor plans and elevations for the model frames. The span length of 9.1 m (30 ft) was used. In floor plans, IMF systems were selected and designed for resisting seismic force as seen in Fig. 1.

Steel material ASTM A992/A992M was used for beams and columns. According to ASCE 7-10 (2010), for IMFs, the response modification factor (*R*), overstrength factor (Ω), and deflection amplification factor (C_d) are 4.5, 3.0, and 4.0, respectively. Members were designed according to AISC 341-10 (2010), and AISC 360-10 (2010). The dead load and live load for member deign were assumed as 4.12 kPa (86 lbs/ft^2) and 0.96 kPa (20 lbs/ft^2), respectively. The basic wind speed of 51 m/sec was used, and surface roughness was assumed as B for urban office buildings [Chapters 26 and 27 in ASCE 7-10 (2010)]. The seismic base shear can be determined as C_S times the weight of the building (*W*). ASCE 7-10 (2010) requires that seismic response coefficient C_S should not be less than the smaller of $0.044S_{DS}I_e$ and 0.01g, where I_e is the importance factor.

Considering all design parameters as mentioned above, four IMFs, which were summarized in Table 1, were designed. The frames were classified into two performance groups according to seismic design categories (SDC C_{min} and SDC C_{max}).

The designed member sections for the different frames are summarized in Table 2~4. For the SDC C_{min} and C_{max} 30 story frames, the member sections were determined by design seismic force whereas member sections of 40

Table 1. Summary of model frames and performance groups

No.	Performance Group	No.	Arch.ID	Bay Size	No. of Stories	Seismic Design Criteria				
						SDC	Mass (ton)	T_n^* (sec)	T_1^* (sec)	C_S^+ (g)
1	Min-x%	1	30CMIN	9.1m (30ft)	30	C_{min}	11324	5.466	3.314	0.015
		2	40CMIN		40		9666	6.863	3.679	0.015
2	Max-x%	3	30CMAX		30	C_{max}	11324	5.018	3.105	0.022
		4	40CMAX		40		9666	6.301	3.679	0.022

T_n^* : Fundamental period (=C_uT_a), T_1^* : 1st mode period, C_S^+ : Seismic response coefficient, x%: connection rotation capacity (1%, 2%, 3% and 4% radian)

story frames building were determined by assumed wind force. For this reason, the member sections of 40 story, unlike 30 story frames, frames were same regardless of seismic design category.

To investigate the effect of connection rotation capacity on the seismic performance of IMFs, moment connections were modeled using rotational spring element with three different rotation capacities: (1) 0.01 rad, (2) 0.02 rad, (3) 0.03 rad and (4) 0.04 rad. To model connections with each rotation capacity, the moment of rotational spring element was suddenly dropped at each rotation (0.01, 0.02, 0.03 and 0.04 rad) to fracture. Since four different connection models for each model frame were used, the number of model frames used for performance evaluation was 12 (=3×4). In Table 1, frame ID 'MIN-2%' represents the IMF with a connection rotation capacity of 0.02 rad, which were designed for seismic loads for SDC C_{min} according to ASCE 7-10 (2010) design seismic forces.

3. Analytical Model for Frames and Moment Connections

For obtaining the reliable results from the seismic performance evaluation, the use of an accurate analytical model is very important. In this study, the IMF and moment connection were modeled using OpenSees (Mazzoni et al., 2007) as shown in Figs. 2 and 3.

Fig. 2 represents the layout of analytical model used in

Table 2. Beam and column sections of 30 story building (SDC C_{min})

Story / Floor	Columns			Girder
	Exterior	Interior	Tube section	
1 / 2	W14X665	W14X808	TS30x30x5/8	W36X232
2~3 / 3~4	W14X398	W14X605	TS30x30x5/8	W36X232
4~5 / 5~6	W14X342	W14X550	TS28x28x5/8	W36X210
6~7 / 7~8	W14X283	W14X500	TS28x28x5/8	W36X182
8~9 / 9~10	W14X257	W14X455	TS28x28x5/8	W36X170
10~11 / 11~12	W14X211	W14X455	TS28x28x5/8	W36X182
12~13 / 13~14	W14X159	W14X398	TS28x28x5/8	W36X150
14~15 / 15~16	W14X132	W14X342	TS28x28x5/8	W36X150
16~17 / 17~18	W14X109	W14X283	TS26x26x5/8	W36X135
18~19 / 19~20	W14X82	W14X257	TS26x26x5/8	W33X130
20~21 / 21~22	W14X82	W14X233	TS26x26x5/8	W30X108
22~23 / 23~24	W14X74	W14X193	TS18x18x5/8	W30X90
24~25 / 25~26	W14X53	W14X159	TS18x18x5/8	W27X84
26~27 / 27~28	W14X43	W14X109	TS16x16x5/8	W24X62
28~29 / 29~30	W14X30	W14X74	TS16x16x3/8	W21X44
30 / Roof	W14X22	W14X34	TS16x4x1/2	W14X26

Table 3. Beam and column sections of 30 story building (SDC C_{max})

Story / Floor	Columns			Girder
	Exterior	Interior	Tube section	
1 / 2	W14X665	W14X808	TS30x30x5/8	W36X232
2~3 / 3~4	W14X398	W14X550	TS30x30x5/8	W36X232
4~5 / 5~6	W14X342	W14X550	TS28x28x5/8	W36X210
6~7 / 7~8	W14X283	W14X500	TS28x28x5/8	W36X182
8~9 / 9~10	W14X257	W14X455	TS28x28x5/8	W36X170
10~11 / 11~12	W14X211	W14X426	TS28x28x5/8	W36X182
12~13 / 13~14	W14X159	W14X398	TS28x28x5/8	W36X150
14~15 / 15~16	W14X132	W14X342	TS28x28x5/8	W36X150
16~17 / 17~18	W14X109	W14X311	TS26x26x5/8	W36X135
18~19 / 19~20	W14X82	W14X311	TS26x26x5/8	W33X130
20~21 / 21~22	W14X82	W14X257	TS26x26x5/8	W30X108
22~23 / 23~24	W14X74	W14X211	TS18x18x5/8	W30X90
24~25 / 25~26	W14X53	W14X145	TS18x18x5/8	W27X84
26~27 / 27~28	W14X43	W14X109	TS16x16x5/8	W24X62
28~29 / 29~30	W14X30	W14X68	TS16x16x3/8	W21X44
30 / Roof	W14X22	W14X38	TS16x4x1/2	W14X26

Table 4. Beam and column sections of 40 story building (SDC C_{min} and C_{max})

Story / Floor	Columns			Girder
	Exterior	Interior	Tube section	
1 / 2	W14X808	W36X798	TS31x31x9/10	W36X256
2~3 / 3~4	W14X730	W14X665	TS31x31x9/10	W36X256
4~5 / 5~6	W14X605	W14X730	TS31x31x4/5	W36X232
6~7 / 7~8	W14X550	W14X605	TS31x31x7/10	W36X232
8~9 / 9~10	W14X500	W14X550	TS31x31x7/10	W36X232
10~11 / 11~12	W14X455	W14X500	TS31x31x7/10	W36X232
12~13 / 13~14	W14X370	W14X500	TS31x31x7/10	W36X232
14~15 / 15~16	W14X283	W14X455	TS31x31x7/10	W36X230
16~17 / 17~18	W14X257	W14X398	TS31x31x7/10	W36X230
18~19 / 19~20	W14X233	W14X398	TS30x30x5/8	W36X230
20~21 / 21~22	W14X193	W14X342	TS30x30x5/8	W36X210
22~23 / 23~24	W14X159	W14X342	TS28x28x5/8	W36X194
24~25 / 25~26	W14X145	W14X257	TS28x28x5/8	W36X170
26~27 / 27~28	W14X132	W14X233	TS26x26x5/8	W36X170
28~29 / 29~30	W36X170	W14X176	TS24x24x5/8	W36X170
30~31 / 31~32	W36X170	W14X159	TS24x24x5/8	W36X170
32~33 / 33~34	W36X170	W14X159	TS24x24x5/8	W36X170
34~35 / 35~36	W33X118	W14X90	TS24x24x5/8	W33X118
36~37 / 37~38	W30X108	W14X90	TS24x24x5/8	W30X108
38~39 / 39~40	W24X94	W14X90	TS16x16x1/2	W24X94
40 / Roof	W24X94	W14X90	TS16x16x1/2	W24X94

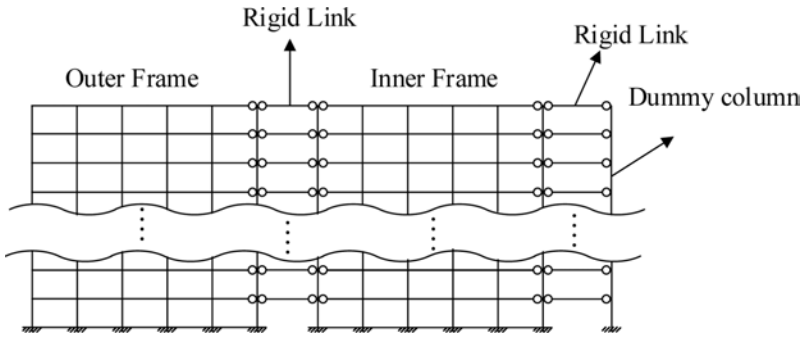

Figure 2. Analysis model of moment frames.

this study. To construct 2D analytical model which is considered both inner and outer frames, the two frames are linked with rigid beam elements as shown Fig. 2. Pins are placed on each end of the rigid beam elements. To account for P-Δ effect, this study use an additional dummy columns for two dimensional analytical model.

The moment connections were modeled as shown Fig. 3. The inelastic behaviors of column and beam member were predicted using the stress-strain relationship assigned for fiber sections. The yield stress was defined as the expected yield strength (RyFy) of members. The slope of strain hardening branch was assumed as 2% of the slope in the elastic range. The interaction between axial forces and moments in columns was also considered in the analytic model. Therefore, moment-rotation relationships for beams and columns were modeled to yield at expected plastic moment capacity of members, and to have bilinear hysteretic behavior as shown in Fig. 3(a) and 3(b).

The fracture springs were modeled using inelastic rotational spring element that was placed at the ends of the beam [Fig. 3(c)]. The fracture springs control the rotation capacity of beam by dropping the strength suddenly when the rotation of the spring reaches its rotation capacity.

4. Seismic Performance Evaluation

FEMA P695 (2009) provided a methodology for quantifying system performance and response parameters for use in seismic design. The two performance objectives used in FEMA P695 (2009) are: (1) The probability of

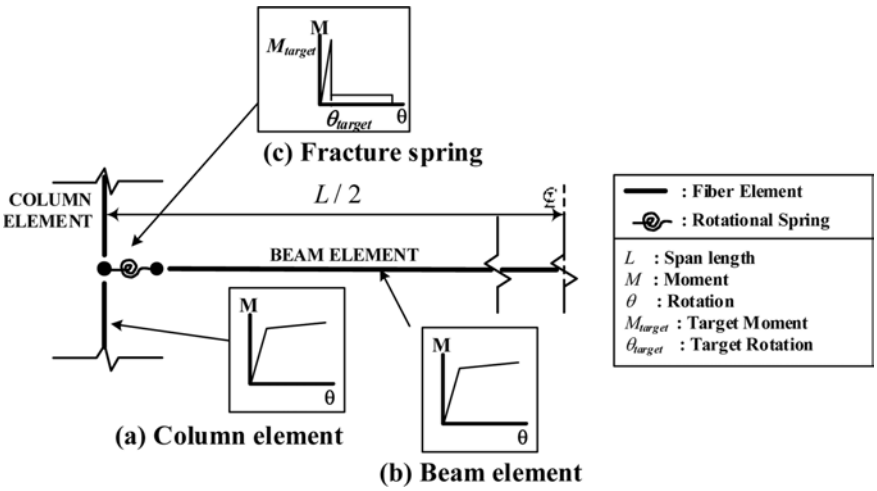

Figure 3. Analysis model of moment connections.

collapse for the maximum considered earthquake (MCE) ground motions is recommended to be 10%, or less on average across a performance group that contains model frames having a specific seismic force resisting system with different configurations, and (2) For an individual model frame, the probability of collapse is 20%, or less. To achieve those objectives, the adjusted collapse margin ratio (*ACMR*) is estimated, and compared with limiting values of ACMR as follows:

(1) The average value ($\overline{ACMR}$) of the adjusted collapse margin ratios for each performance group exceeds $ACMR_{10\%}$:

$$\overline{ACMR} \geq ACMR_{10\%} \tag{1}$$

(2) The individual value ($ACMR_i$) of the adjusted collapse margin ratios of model frames in a performance group exceeds $ACMR_{20\%}$:

$$ACMR_i \geq ACMR_{20\%} \tag{2}$$

The values of $ACMR_{10\%}$ and $ACMR_{20\%}$ correspond to collapse probabilities of 10 and 20%, respectively. A step-by-step procedure to determine $\overline{ACMR}$ and $ACMR_i$ for the performance group and individual model frame is as follows:

① Select the model frames having a specific seismic force resisting system of interest which reflects the range of design variables such as number of stories s, bay lengths, and seismic design categories (SDCs), and design the selected frames according to current seismic design provisions. Classify the model frames into performance groups that share a common set of features and behavior characteristics.

② Idealize the model frame using a proper analytical model.

③ Conduct nonlinear static analysis to determine the overstrength factor, Ω, and period-based ductility, μ_T (=δ_u/δ_{yeff}) using Eqs. (3) and (4) with Eq. (5), respectively. [Fig. 7(a)]

$$\Omega = \frac{V_{max}}{V_d} \tag{3}$$

$$\mu_T = \frac{\delta_u}{\delta_{yeff}} \tag{4}$$

$$\delta_{y,eff} = C_0 \frac{V_{max}}{W}\left[\frac{g}{4\pi^2}\right](\max(T_n, T_1))^2 \tag{5}$$

where V_{max} is the maximum base shear resistance, V_d is the design base shear, δ_u is the roof drift displacement at the point of 20% strength loss (=0.8V_{max}), δ_{yeff} is the effective yield roof displacement, C_0 relates the displacement of the single degree of freedom system at the fundamental mode of frame to the roof displacement of the frame, g is the gravity constant, T_n is the fundamental period defined as C_uT_a specified in ASCE 7-10 (2010), and T_1 is the fundamental period of the model frame computed by using eigenvalue analysis.

④ Conduct the incremental dynamic analysis (IDA) for computing median collapse capacity, $\hat{S}_{CT}$ (Han and Chopra, 2006; Vamvatsikos and Cornell, 2002), and calculate the collapse margin ratio, *CMR*, for each model frame. Collapse is defined as the global dynamic instability as specified in FEMA P695 (2009). When the frame reaches the dynamic instability state, deformation (e.g., story drift) increases without bound according to the slight increase in ground motion intensity which can be represented by pseudo spectral acceleration [$PSA(T_n, 5\%)$] at the fundamental period (T_n) of a 5% damped SDF system. The *CMR* is calculated using Eq. (6):

$$CMR = \frac{\hat{S}_{CT}}{S_{MT}} \tag{6}$$

where S_{MT} is $PSA(T_n, 5\%)$ at T_n of a model frame corresponding to the maximum considered earthquake at a site of interest.

⑤ Calculate the spectral shape factor (*SSF*) that accounts for the spectral shape of rare ground (Baker and Cornell, 2006), and adjust the *CMR*.

$$SSF = \exp[\beta_1(\bar{\varepsilon}_o(T) - \bar{\varepsilon}(T))_{record}] \quad (7)$$

$$\bar{\varepsilon}_o(T)_{record} = 0.6(1.5 - T) \quad (8)$$

$$\beta_1 = 0.14(\mu_T - 1)^{0.42} \quad (9)$$

where $\bar{\varepsilon}_o$ is 1.0 for SDC B and C, 1.5 for SDC D, and 1.2 for SDC E.

⑥ Calculate the *ACMR*:

$$ACMR = CMR \times SSF \quad (10)$$

⑦ Calculate ACMR10% and ACMR20%:

$$ACMR_{10\%} = \exp[-\beta_{ToT} \times \Phi^{-1}(0.1)] \quad (11)$$

$$ACMR_{20\%} = \exp[-\beta_{ToT} \times \Phi^{-1}(0.2)] \quad (12)$$

where $\Phi^{-1}(x)$ is the inverse of the cumulative distribution function of the standard normal variate x and β_{TOT} is the total system collapse uncertainty calculated using Eq. (13):

$$\beta_{TOT} = \sqrt{\beta_{RTR}^2 + \beta_{DR}^2 + \beta_{TD}^2 + \beta_{MDL}^2} \quad (13)$$

where β_{RTR} is the record-to-record uncertainty ($0.2 \le \beta_{RTR} = 0.1 + 0.1\mu_T \le 0.4$),and β_{DR}, β_{TD} and β_{MDL} are the design requirement-related uncertainty, test data-related uncertainty and modeling uncertainty, respectively, ranging from 0.1 to 0.5 that can be determined from the tables in pages 3-8, 3-20, and 5-23 of FEMA P695 (2009). This study adopted the values of uncertainties in Eq. (13) provided by FEMA P-695 (2009), which correspond to low accuracy and robustness in analysis and prediction.

⑧ Determine whether individual model frames and the performance group satisfy the acceptable performance criteria specified in Eqs. (1) and (2).

5. Seismic Performance of IMFs according to Different Rotation Capacities of Connections

IDA curves are obtained from incremental dynamic analysis (IDA), requiring repeated nonlinear response history analyses of the structure for an ensemble of ground motions, each scaled to many intensity levels, selected to cover the entire range of structural response from elastic behavior to global dynamic instability. The IDA curves are examined to evaluate the collapse capacity of the model frames.

Figs. 4 and 5 show the IDA curves of high-rise IMF systems. The abscissa and ordinate of IDA curves are maximum interstory drift (θ_{max}) and pseudo spectral acceleration at the fundament period (T_n) of a 5% damped system [$PSA(T_n, 5\%)$], respectively. Although the member sections of 40 story frames for C_{min} and C_{max} were same regardless of SDC, difference in the fundamental periods (T_n) between two 40 story frames leads to difference in $PSA(T_n,5\%)$s. So, as shown in Fig. 5, the results of IDA for the 40-story IMFs are different. Collapse capacities and median collapse capacities can be obtain from IDA curves (Figs. 4, 5) and the *CMR* can be calculated using Eq. (6).

In IDA curves of IMF systems, the slope of the IDA curves in the elastic response range of the frames is similar among IMF systems having the different rotation capacity. In the post-fracture response range, the slope of the IDA curves for the model frame whose maximum interstory drift ratio reaches the rotation capacity decreases significantly, whereas the slope of the IDA curve for the corresponding frames having higher rotation capacity do not deteriorate. It can be also seen that most of the IMFs collapsed after occurring moment connection fracture with a little increase of resistance strength.

For 30 story frames, *CMR*s of the frames which have lower rotation capacity at moment connections are nearly 1 as shown in Fig. 4. It shows that these frames with lower rotation capacity are significantly more vulnerable on seismic performance capacities than those with higher rotation capacity. In particular, *CMRs* of the C_{max} frames were lower than that of the C_{min} frames.

Although 40 story frames are higher building than 30 story frames, the CMR values were higher than those of 30 story frames as shown in Fig. 5. This is because, as mentioned above, the member sections of 40 story frames were determined by the wind force rather than seismic force and so they showed better seismic capacity than 30 story frames. *CMR* of the C_{max} frames for 40 story frames were lower than that of the C_{min} frames too, as well as 30 story frames.

Fig. 6 shows median IDA curves for model frame extracted from 44-IDA curves (one for each of the 44 ground motions considered in this study). As shown in the figure, the slopes of each IDA curve decreased since maximum interstory drift ratios reached at rotation capacity (θ_F). Solid circle in Fig. 7 represent the point where connection fracture occurs for the first time in the model frames. The strength and drift at connection fracture are denoted by $\hat{S}_{FT}$ [the median strength, $PSA(T_n, 5\%)$] and θ_F, respectively.

When subjected to design seismic intensity (S_{MT}), the maximum interstory drift ratio of 30 story frames for SDC C_{min} and C_{max} was observed at approximately 0.02 rad and 0.03 rad, respectively. For 40 story frames, the maximum interstory drift ratio for SDC C_{min} and C_{max} was observed at approximately 0.01 rad and 0.02 rad, respectively. The

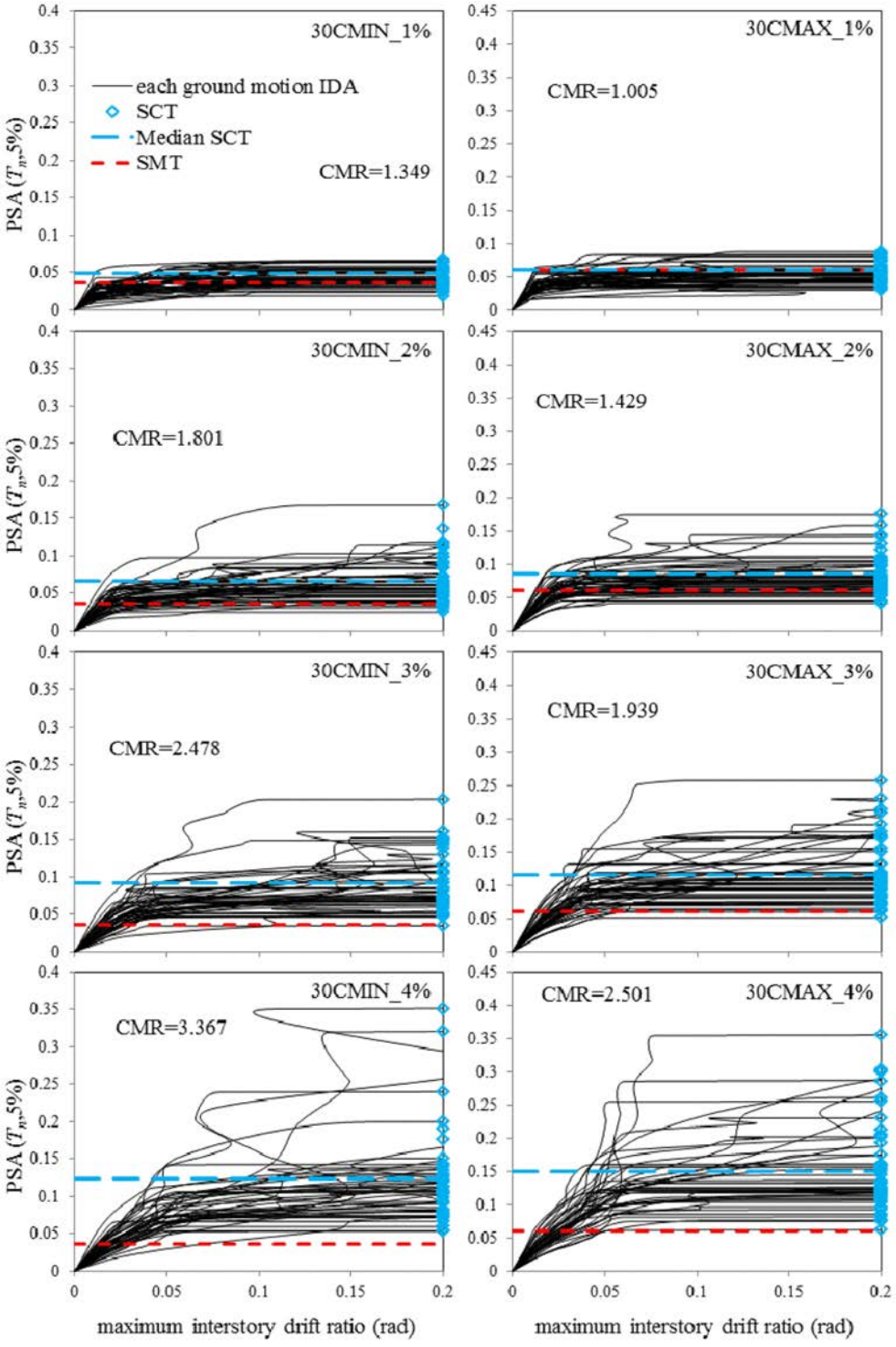

Figure 4. IDA curves of 30 story IMF systems.

reason that CMR for 30 story frames with lower rotation capacity was almost 1 is that rotation connections fractured under seismic intensity less than S_{MT}.

This study evaluated ratios between design seismic intensity (S_{MT}) and strength at connection fracture. Fig. 7 shows the values of the $\hat{S}_{CT}/\hat{S}_{FT}$ ratio for the model frames. The $\hat{S}_{CT}/\hat{S}_{FT}$ ratio represents the reserve strength in frames after connection fracture. The differences in $\hat{S}_{CT}/\hat{S}_{FT}$ ratios were not significant for all the frames. However, $\hat{S}_{CT}/\hat{S}_{FT}$ ratios for 30 story frames were slightly decreased with increasing rotation capacity with average value of 1.89, whereas the ratios for 40 story frames were

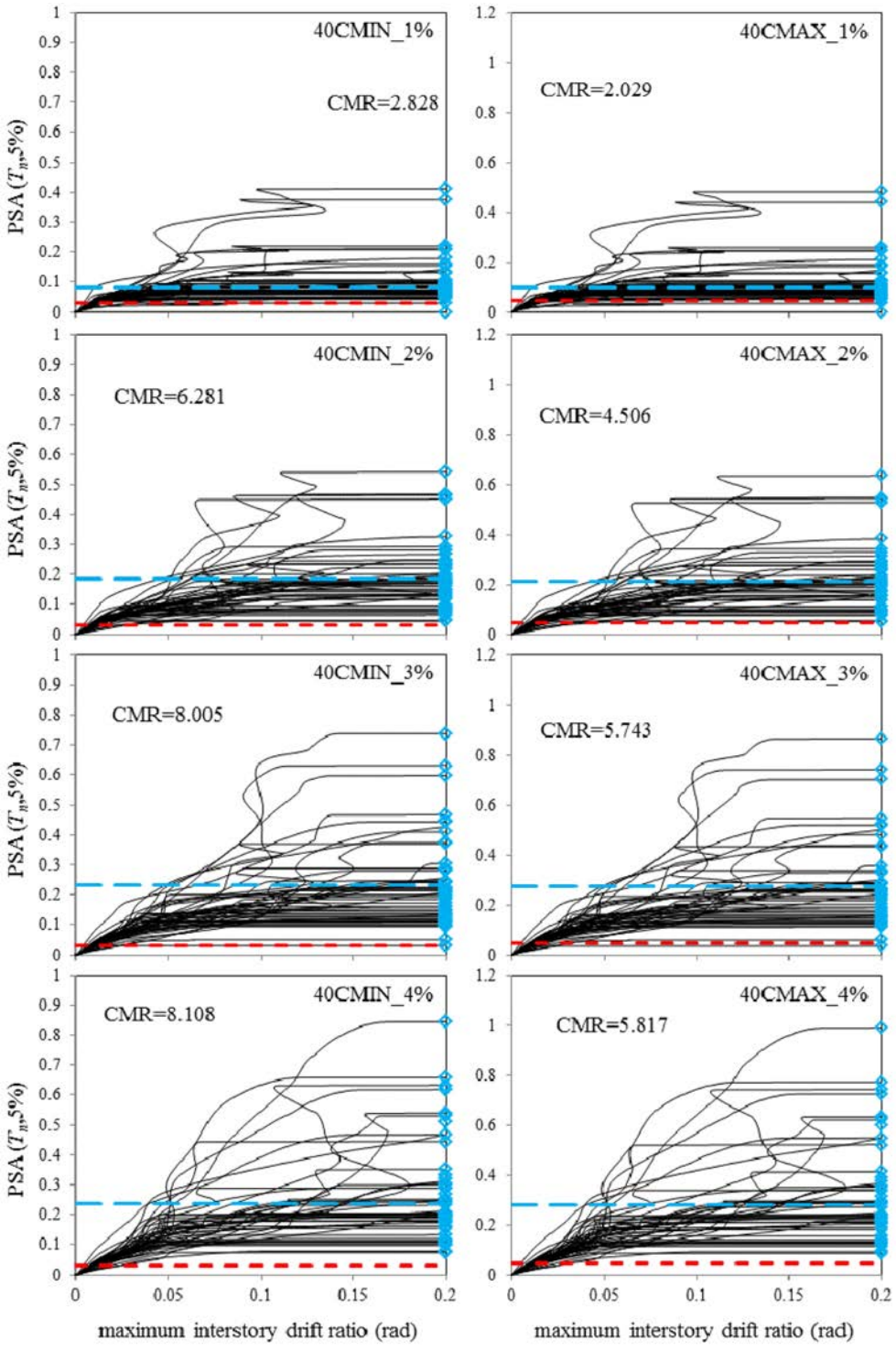

Figure 5. IDA curves of 40 story IMF systems.

increased with increasing rotation capacity with average value of 2.63 which was higher than those of 30 story frames.

Seismic performance evaluation is conducted for the model frames using the procedure prescribed in FEMA P 69 (2009). Table 5 summarizes the evaluation results for each model frame. As shown Table 5, 30 story IMF frame in SDC C_{max} fail to meet the FEMA P695 (2009) acceptance criteria though the rotation capacity of that have 0.02 radian which is minimum rotation capacity of moment connection for IMF system.

In order to investigate the effects of the rotation capacity

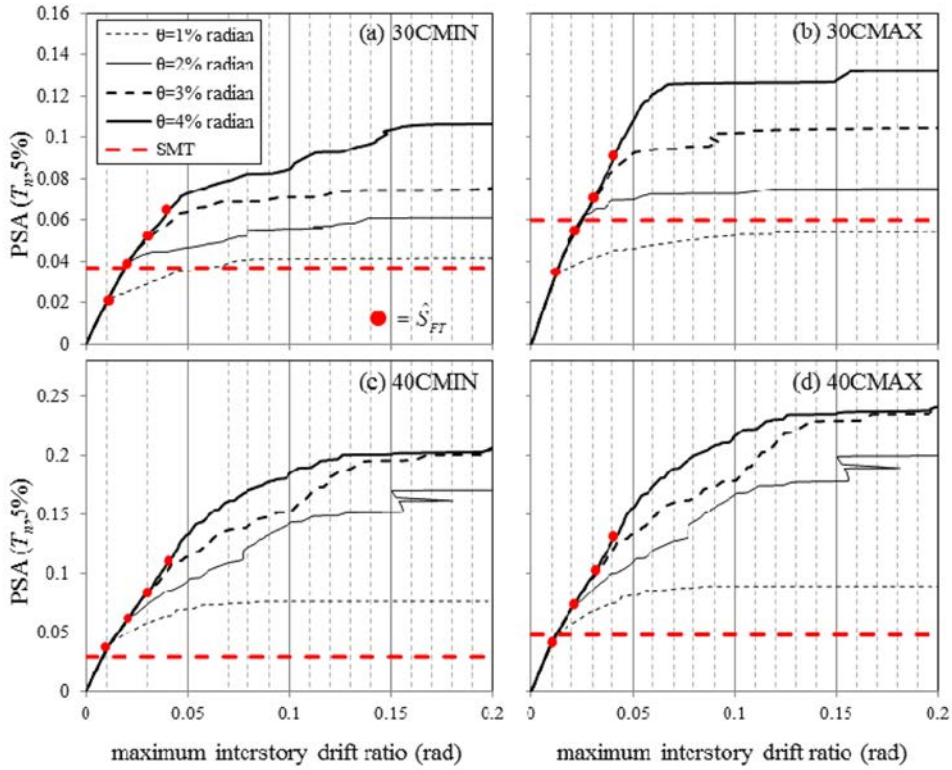

Figure 6. Median IDA curves of 30 story and 40 story IMF systems.

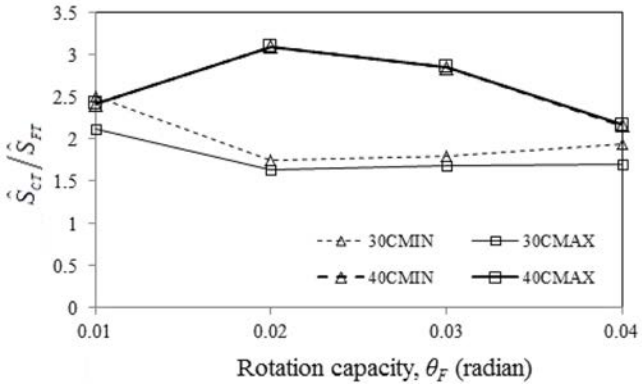

Figure 7. $\hat{S}_{CT}/\hat{S}_{FT}$ values according to rotation capacity, θ_F.

on the probability of collapse subjected to maximum considered earthquake, the probability of collapse [$P(collapse \mid S_{MT})$] for each model frame is calculated using Eq. (14).

$$P(collapse|S_{MT}) = P(S_{CT} < S_{MT}) = \Phi\left(\frac{\ln S_{MT} - \ln \hat{S}_{CT}}{\beta_{TOT}}\right) \quad (14)$$

Fig. 8 shows the probability of collapse with respect to different rotation capacity.

The probability of collapse becomes higher with a decrease in rotation capacity. The probability of collapse for 40 story IMF systems satisfied the allowable probability of collapse presented in FEMA P695 (2009) from the IMF having 0.01 radian rotation capacity. However, the probability of collapse for 30 story IMF systems in SDC C_{max} satisfied the allowable probability of collapse presenting in FEMA P695 (2009) from the IMF having 0.03 radian rotation capacity.

In summary, when member sections for high-rise structure are determined by wind loads not seismic loads, the structures satisfy the FEMA P695 (2009) criteria when their connections had a rotation capacity of 0.02 radian or larger. However, for high-rise structures that member sec-

Table 5. Summary of collapse margin parameters and acceptance check

No.	Performance Group	No.	Arch.ID	Computed Overstrength and Collapse Margin Parameters							Acceptance Check		
				S_{MT}		T	S_{CT}	CMR	SSF	ACMR	TOT	Accept. ACMR	Pass/Fail
		1	30CMIN	0.037	4.807	1.270	0.049	1.35	1.08	1.46	0.65	1.72	Fail
1	Min-1%	2	40CMIN	0.029	7.098	1.000	0.082	2.83	1.00	2.83	0.64	1.71	Pass
		Average			**5.952**	**1.135**		**2.09**		**2.14**	**0.64**	**2.28**	**Fail**
		3	30CMAX	0.060	4.254	1.616	0.060	1.00	1.12	1.13	0.66	1.74	Fail
2	Max-1%	4	40CMAX	0.048	4.685	1.060	0.097	2.03	1.04	2.12	0.64	1.71	Pass
		Average			**4.469**	**1.338**		**1.52**		**1.62**	**0.65**	**2.30**	**Fail**
		5	30CMIN	0.037	7.009	1.409	0.066	1.80	1.10	1.98	0.65	1.73	Pass
3	Min-2%	6	40CMIN	0.029	11.406	1.018	0.183	6.28	1.03	6.45	0.64	1.71	Pass
		Average			**9.207**	**1.214**		**4.04**		**4.21**	**0.65**	**2.29**	**Pass**
		7	30CMAX	0.060	5.418	1.360	0.085	1.43	1.10	1.57	0.65	1.73	Fail
4	Max-2%	8	40CMAX	0.048	7.528	1.209	0.215	4.51	1.08	4.84	0.65	1.72	Pass
		Average			**6.473**	**1.284**		**2.97**		**3.21**	**0.65**	**2.29**	**Pass**
		9	30CMIN	0.037	7.831	1.529	0.091	2.48	1.11	2.76	0.66	1.74	Pass
5	Min-3%	10	40CMIN	0.029	12.979	1.091	0.233	8.01	1.05	8.43	0.64	1.72	Pass
		Average			**10.405**	**1.310**		**5.24**		**5.59**	**0.65**	**2.30**	**Pass**
		11	30CMAX	0.060	6.045	1.589	0.116	1.94	1.12	2.17	0.66	1.74	Pass
6	Max-3%	12	40CMAX	0.048	8.566	1.295	0.273	5.74	1.09	6.25	0.65	1.73	Pass
		Average			**7.306**	**1.442**		**3.84**		**4.21**	**0.65**	**2.31**	**Pass**
		13	30CMIN	0.037	8.797	2.123	0.123	3.37	1.16	3.90	0.68	1.78	Pass
7	Min-4%	14	40CMIN	0.029	13.988	1.292	0.236	8.11	1.09	8.81	0.65	1.73	Pass
		Average			**11.393**	**1.708**		**5.74**		**6.36**	**0.67**	**2.34**	**Pass**
		15	30CMAX	0.060	6.435	1.807	0.150	2.50	1.14	2.84	0.67	1.75	Pass
8	Max-4%	16	40CMAX	0.048	9.232	1.533	0.277	5.82	1.11	6.48	0.66	1.74	Pass
		Average			**7.833**	**1.670**		**4.16**		**4.66**	**0.66**	**2.34**	**Pass**

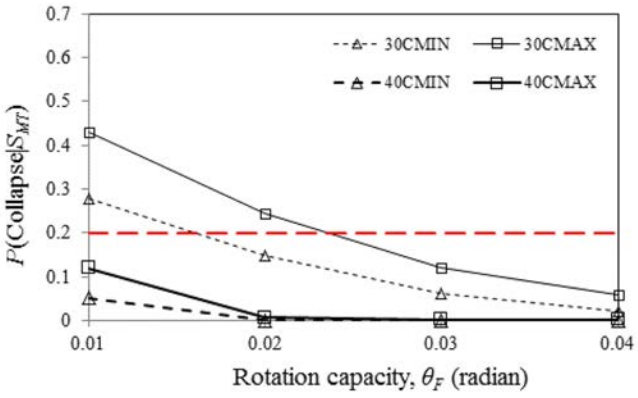

Figure 8. Probability of collapse for MCE earthquake with respect to rotation capacity.

tions are determined by seismic loads, their rotation capacity of moment connection should be larger than 0.03 rad to satisfy the criteria.

6. Conclusion

This study evaluated the seismic performance of high-rise steel intermediate moment frames designed considering current seismic design provisions. For seismic performance evaluation of high-rise IMFs, four IMFs were designed with seismic design category C_{min} and C_{max}. The member sections of 30-story frames were determined by seismic loads, whereas those of 40 story-frames were determined by wind loads. The seismic performance evaluation (FEMA P695, 2009) was conducted with IMF considering four different connection rotation capacities. The conclusions are summarized as follows:

(1) The Collapse margin ratio (CMR) of the 40 story

frames is higher than that of the 30 story frames. With a decrease in SDC, the CMR value became larger. The thirty story IMF designed for SDC C_{max} had the smallest CMR among all model IMF frames.

(2) This study evaluated a ratio of median collapse strength and connection fracture strength, $\hat{S}_{CT}/\hat{S}_{FT}$. The values were slightly increase with increasing rotation capacity. Thirty-story IMFs had a lower $\hat{S}_{CT}/\hat{S}_{FT}$ ratio than the 40-story frames.

(3) The 30-story IMFs designed for C_{max} with a rotation capacity of 0.02 rad did not satisfy the required seismic performance specified in FEMA P-695. The rotation capacity of 30 story IMFs should not be less than 0.03 radian to satisfy the performance criteria in FEMA P695 (2009).

(4) If the member sections in IMFs were determined by wind loads rather than seismic loads, the seismic performance of IMFs with connections having a rotation capacity of 0.02 rad meet the performance criteria specified in FEMA P695(2009). However, when seismic loads governed, IMFs with connections having a rotation capacity of 0.02 rad did not meet the performance criteria. Therefore, the rotation capacity of moment connections in high rise IMFs shall not be less than 0.03 radian.

Acknowledgments

Authors acknowledge the financial supports provided by National research foundation of Korea (No. 2014R1 A2A1A11049488).

References

American Institute of Steel Construction (AISC). (2010). “Seismic provisions for structural steel buildings.” ANSI/AISC 341-10. Chicago, IL.

American Institute of Steel Construction (AISC). (2010). “Specification for Structural Steel Buildings.” ANSI/AISC 360-10. Chicago, IL.

American Society of Civil Engineers (ASCE). (2010). “Minimum design loads for buildings and other structures.” ASCE/SEI 7-10. Reston, VA

Baker, J. W. and Cornell, C. A. (2006). “Spectral shape, epsilon and record selection.” *Journal of Earthquake Engineering and Structural Dynamics*, 35, pp. 1077~1095.

FEMA. (2000). “State of the Art Report on Past Performance of Steel Moment-Frame Buildings in Earthquakes.” FEMA 355E. SAC Joint Venture and FEMA. Washington, DC.

FEMA. (2000). “State of the Art Report on Performance Prediction and Evaluation of Steel Moment-Frame Buildings.” FEMA 355F. SAC Joint Venture and FEMA. Washington, DC.

FEMA. (2000). “State of the Art Report on Systems Performance of Steel Moment Frames Subject to Earthquake Ground Shaking.” FEMA 355C. SAC Joint Venture and FEMA. Washington, DC.

FEMA. (2009). “Quantification of Building Seismic Performance Factors.” FEMA P695. SAC Joint Venture and FEMA. Washington, DC.

Han, S. W. and Chopra, Anil K. (2006). “Approximate incremental dynamic analysis using the modal pushover analysis procedure.” *Journal of Earthquake Engineering and Structural Dynamics*, 35(15), pp. 1853~1873.

Han, S. W., Moon, K. H., Hwang, S. H., and Stojadinovic, B. (2013.) “Seismic Performance Evaluation of Intermediate Moment Frames with Reduced Beam Section and Bolted Web Connections.” Earthquake Spectra. In-Press.

Mazzoni, S., McKenna, F., Scott, M. H., and Fenves, G. L. (2007). “OpenSees command language manual.” The Univ. of California. Berkeley, Calif. Available from: http://opensees.berkeley.edu/index.php

Vamvatsikos, D. and C. Allin Cornell. (2002). “Incremental dynamic analysis.” *Journal of Earthquake Engineering and Structural Dynamics*, 31(3), pp. 491~514.